THE JOURNAL OF BIOLOGICAL CHEMISTRY Vol. 276, No. 46, Issue of November 16, pp. 42807–42811, 2001
*Printed in U.S.A.*

# Optimization of Receptor-G Protein Coupling by Bilayer Lipid Composition II

## FORMATION OF METARHODOPSIN II-TRANSDUCIN COMPLEX*

Received for publication, June 21, 2001, and in revised form, August 22, 2001
Published, JBC Papers in Press, September 5, 2001, DOI 10.1074/jbc.M105778200

**Shui-Lin Niu, Drake C. Mitchell, and Burton J. Litman‡**

*From the Section of Fluorescence Studies, Laboratory of Membrane Biochemistry and Biophysics, National Institute on Alcohol Abuse and Alcoholism, Rockville, Maryland 20852*

**The visual transduction system was used as a model to investigate the effects of membrane lipid composition on receptor-G protein coupling. Rhodopsin was reconstituted into large, unilamellar phospholipid vesicles with varying acyl chain unsaturation, with and without cholesterol. The association constant ($K_a$) for metarhodopsin II (MII) and transducin ($G_t$) binding was determined by monitoring MII-$G_t$ complex formation spectrophotometrically. At 20 °C, in pH 7.5 isotonic buffer, the strongest MII-$G_t$ binding was observed in 1-stearoyl-2-docosahexaenoyl-*sn*-glycero-3-phosphocholine (18:0,22:6PC), whereas the weakest binding was in 1-stearoyl-2-oleoyl-*sn*-glycero-3-phosphocholine (18:0,18:1PC) with 30 mol% cholesterol. Increasing acyl chain unsaturation from 18:0,18:1PC to 18:0,22:6PC resulted in a 3-fold increase in $K_a$. The inclusion of 30 mol% cholesterol in the membrane reduced $K_a$ in both 18:0,22:6PC and 18:0,18:1PC. These findings demonstrate that membrane compositions can alter the signaling cascade by changing protein-protein interactions occurring predominantly in the hydrophilic region of the proteins, external to the lipid bilayer. These findings, if extended to other members of the superfamily of G protein-coupled receptors, suggest that a loss in efficiency of receptor-G protein binding is a contributing factor to the loss of cognitive skills, odor and spatial discrimination, and visual function associated with *n*-3 fatty acid deficiency.**

The G protein-coupled motif is a fundamental mode of cell signaling, utilized in vision, taste, olfaction, and a variety of neurotransmitter systems. The receptors for these systems are integral membrane proteins, embedded in a lipid matrix. Neuronal and retinal tissues and the olfactory bulb contain high levels of the *n*-3 polyunsaturated acyl chain derived from docosahexaenoic acid (22:6*n*-3)[1] in their cell membrane phospholipids (1, 2). Approximately 50% of the acyl chains in the phospholipids of the ROS disc membrane consist of 22:6*n*-3 (1). The physiological significance of 22:6*n*-3 is demonstrated by the impaired visual response (3), learning deficits (2), loss of odor discrimination (4), and reduced spatial learning (5) associated with n-3 fatty acid deficiency. In all cases where acyl chain analysis was carried out, the 22:6*n*-3 content of membrane phospholipids was dramatically reduced in the *n*-3-deficient animals where it was replaced by 22:5*n*-6 (5). These findings suggest that the high levels of 22:6*n*-3 in membrane phospholipids play a critical role in various membrane-associated signaling pathways. A common thread in several of these processes is the ubiquitous motif of G protein-coupled signaling systems. However, molecular mechanisms linking 22:6*n*-3 phospholipids with essential physiological functions remain to be clarified. The study described herein aims to elucidate such mechanisms by investigating the effect of membrane lipid composition on G protein-coupled signal transduction.

In G protein-coupled systems, the receptor activates an effector protein through the action of a G protein (6). Receptors in this superfamily are integral membrane proteins made up of seven transmembrane helices and their respective connecting loops. In contrast, the G protein and effector proteins are generally peripheral proteins, bound to the membrane by a combination of an isoprenoid chain-lipid bilayer interactions (7, 8) and electrostatic forces (9). The receptor-binding site for the ligand is formed by the transmembrane helices and lies near the midpoint of the membrane; hence, the conformational changes accompanying receptor activation would be expected to have a dependence on the membrane lipid composition. In contrast, the interaction of the G protein with the receptor occurs primary external to the membrane bilayer (10, 11). How the lipid composition might affect the interaction between receptor and G protein external to membrane bilayer is not clear.

The visual transduction system is among the best characterized G protein-coupled signaling systems (12) and is used as a model in these studies (13, 14). Light absorption results in the generation of a rapid equilibrium between MI and MII (15), and the active conformation, MII, readily associates with $G_t$, forming the MII-$G_t$ complex, which is relatively stable in the absence of GTP (16). The interaction sites on MII involved in binding $G_t$ are composed of three cytoplasmic loops formed by the peptide sequence connecting helices III and IV, V and VI, and a putative loop formed by amino acids 310–321, anchored in the bilayer by palmitate groups esterified to Cys-322 and Cys-323 (17–19). Recent structural studies of these loops indicate a level of secondary structure in the form of $\alpha$-helices (20).

* The costs of publication of this article were defrayed in part by the payment of page charges. This article must therefore be hereby marked "*advertisement*" in accordance with 18 U.S.C. Section 1734 solely to indicate this fact.

‡ To whom correspondence should be addressed: Section of Fluorescence Studies, Laboratory of Membrane Biochemistry and Biophysics, National Institute on Alcohol Abuse and Alcoholism, Park 5, Rm. 158, 12420 Parklawn Dr., Rockville, MD 20852. Tel.: 301-594-3608; Fax: 301-594-0035; E-mail: litman@helix.nih.gov.

[1] The abbreviations used are: 22:6*n*-3, docosahexanoic acid, or DHA; 22:5*n*-6, docosapentaenoic acid, or DPA; di22:6PC, 1,2-didocosahexaenoyl-*sn*-glycero-3-phosphocholine; 18:0,22:6PC, 1-stearoyl-2-docosahexaenoyl-*sn*-glycero-3-phosphocholine; 18:0,18:1PC, 1-stearoyl-2-oleoyl-s*n*-glycero-3-phosphocholine; $G_t$, transducin; $K_a$, association constant for MII-$G_t$; $K_{eq}^{-G}$, equilibrium constant for MI-MII in the absence of $G_t$; $K_{eq}^{+G}$, observed equilibrium constant for MI-MII in the presence of $G_t$; MI, metarhodopsin I; MII, metarhodopsin II; ROS, rod outer segment; Rh*, bleached rhodopsin; PS, phosphatidylserine; PE, phosphatidylethanolamine; PC, phosphatidylcholine.

$G_t$ is a trimeric protein consisting of G$\alpha$, G$\beta$, and G$\gamma$ subunits (17). Studies using various peptides representing the putative binding region of $G_t$ implicate two regions in the carboxyl-terminal region of G$\alpha$ and a segment of G$\gamma$ as the interaction sites with MII (18, 19, 21). The interactions appear to be mainly hydrophilic in nature, because the interaction sites are located external to the membrane bilayer.

In this study, rhodopsin was reconstituted into large, unilamellar vesicles containing either di22:6PC, 18:0,22:6PC, or 18:0,18:1PC with and/or without 30 mol% cholesterol and the association constants of MII-$G_t$ formation in these lipids were determined. Our results show that acyl chain unsaturation and cholesterol in the membrane significantly alter the MII-$G_t$ coupling. Because the visual signaling system is the prototype member in the superfamily of G-protein coupled signaling systems, our findings of the effect of lipid composition and cholesterol on receptor-G protein coupling should serve as a general demonstration of the modulation of cell signaling efficiency by membrane composition.

## EXPERIMENTAL PROCEDURES

*Sample Preparation*—Rhodopsin was purified and reconstituted into vesicles consisting of di22:6PC, 18:0,22:6PC, and 18:0,18:1PC with and without cholesterol at a rhodopsin:phospholipid molar ratio of 1:100 as described elsewhere (32).

*Measurement of MII-$G_t$ Binding*—The association constant of MII-$G_t$ was determined spectroscopically, utilizing the fact that MII and MII-$G_t$ have identical absorption spectra (22). MII-$G_t$ complex formation is reflected as an intensity increase at the MII absorption band. The MI-MII equilibrium spectra in the absence and presence of $G_t$ were collected and subsequently deconvolved to obtain the concentrations of MI, MII, MII-$G_t$, and $K_a$.

Rhodopsin-containing vesicles were pre-associated with $G_t$ (0–2 $\mu$M) under isotonic conditions in dark for 4 h on ice. The sample mixtures were then used for spectroscopic measurements as described by Straume *et al.* (23). Briefly, a total of four sequential spectra were recorded for each sample: 1) following equilibration in isotonic buffer, pH 7.5 at 20 °C in the dark; 2) 3 s after partial bleaching (20–30%) by a flash lamp equipped with a 520-nm band pass filter; 3) 10 min after incubation with 30 mM hydroxylamine; and 4) following full bleaching. These spectra were used to calculate the MI-MII equilibrium difference spectra, which were subsequently deconvolved into concentrations of MI, MII, and MII-$G_t$ as described in the following section.

*Data Analysis*—The following equilibria represent the events subsequent to the light activation of rhodopsin in the absence and presence of $G_t$.

$$\text{MI} \leftrightarrow \text{MII}$$

REACTION 1

$$\text{MI} + G_t \leftrightarrow \text{MII} + G_t \leftrightarrow \text{MII-}G_t$$

REACTION 2

Equilibrium difference spectra, which had been corrected for the presence of unbleached rhodopsin, were deconvolved into two Gaussian peaks at ~385 and 480 nm (23). The peak at 480 nm represents MI in both situations, whereas the peak at 385 nm represents MII in the absence of $G_t$ and MII + MII-$G_t$ in the presence of $G_t$. The heights of the 385- and 480-nm bands adjusted with the respective molar extinction coefficients for MII and MI were used to calculate the equilibrium constants $K_{eq}^{-G}$ and $K_{eq}^{+G}$, which are expressed as $K_{eq}^{-G}$ = [MII]/[MI] and $K_{eq}^{+G}$ = ([MII] + [MII-$G_t$])/[MI]. The final parameter obtained from the spectral analysis is the concentration of bleached rhodopsin, [Rh*]. $K_a$ is expressed as shown in Equation 1.

$$1/K_a = [\text{MII}]\cdot[G]_{free}/[\text{MII-}G_t] \quad \text{(Eq. 1)}$$

This can also be written as shown in Equation 2, where $[\text{MII}]_{total}$ = [MII] + [MII-$G_t$], [MII] is the free or unbound MII, and [MII-$G_t$] is the complex of MII to $G_t$.

$$[\text{MII-}G_t]/[\text{MII}]_{total} = [G]_{free}/(1/K_a + [G]_{free}) \quad \text{(Eq. 2)}$$

It has been shown that only half of the rhodopsin is available to interact with G protein in reconstituted vesicles because of the symmetrical distribution of rhodopsin in vesicles (24). The following equations were used to calculate [MII-$G_t$], [MII], and $[G]_{free}$ with consideration of this fact.

$$[\text{MII}] = \tfrac{1}{2}[\text{Rh*}]\cdot K_{eq}^{-G}\cdot(2K_{eq}^{-G} - K_{eq}^{+G} + 1)/\{(1 + K_{eq}^{-G})(1 + K_{eq}^{+G})\} \quad \text{(Eq. 3)}$$

$$[\text{MII-}G_t] = [\text{Rh*}]\cdot(K_{eq}^{+G} - K_{eq}^{-G})/(1 + K_{eq}^{+G}) \quad \text{(Eq. 4)}$$

$$[G]_{free} = [G] - [\text{Rh*}](K_{eq}^{+G} - K_{eq}^{-G})/(1 + K_{eq}^{+G}) \quad \text{(Eq. 5)}$$

Rh* is the amount of bleached rhodopsin.

For each lipid composition, $[\text{MII-}G_t]/[\text{MII}]_{total}$ was analyzed as a function of $[G]_{free}$ and $K_a$ was determined according to Equation 2.

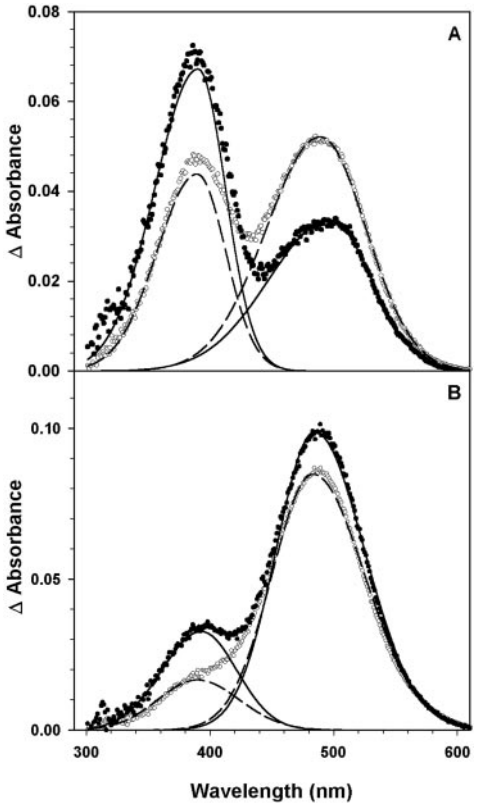


FIG. 1. **Lipid dependence of MII and MII-$G_t$ complex formation.** Spectra were acquired from samples of reconstituted rhodopsin in 18:0,22:6PC vesicles (*panel A*) and 18:0,18:1PC with 30 mol% cholesterol vesicles (*panel B*) in TBS buffer at 20 °C, pH 7.5. Difference equilibrium spectra of MI and MII corrected for the presence of unbleached rhodopsin are shown: ○, in the absence of $G_t$; ●, in the presence of 1 $\mu$M $G_t$. Smooth curves are deconvolved spectra with two absorption peaks at 385 and 480 nm according to "Experimental Procedures:" - - - in the absence of $G_t$ and —— in the presence of $G_t$. The increase in absorbance at 385 nm in the presence of $G_t$ indicates the formation of MII-$G_t$ complex.

## RESULTS

The MI-MII equilibrium and the association of MII with $G_t$ can be readily monitored through changes in the absorption spectra of these photointermediates. Examples of the effect of two different lipid compositions on the MI-MII equilibrium and MII-$G_t$ complex formation are shown in Fig. 1. The spectra for rhodopsin reconstituted in vesicles consisting of a highly unsaturated 18:0,22:6PC are shown in Fig. 1*A*, whereas those in a monounsaturated 18:0,18:1PC mixed with 30 mol% cholesterol are shown in Fig. 1*B*. In the absence of $G_t$, the spectra in Fig. 1*A* contained two absorption bands centered about 385 and 480 nm, associated with the MII and MI photointermediates, respectively. In Fig. 1*A* (*open circles*), the MI and MII peaks are approximately equal, whereas the MII peak was greatly reduced accompanied by a large increase in the MI peak in Fig. 1*B* (*open circles*). The presence of $G_t$ caused an enhancement of

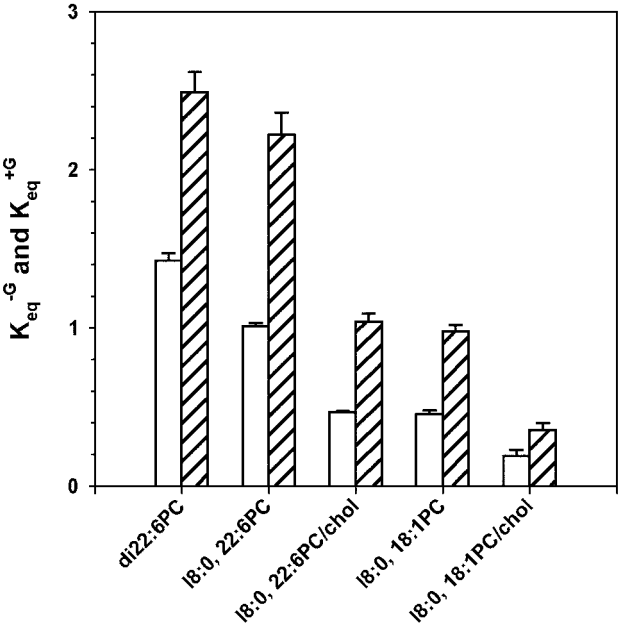


FIG. 2. **Effect of lipid composition on $K_{eq}^{-G}$ (*open bars*) and $K_{eq}^{+G}$ (*diagonal bars*).** These values were derived from equilibrium measurements in the absence and presence of 1.0 $\mu$M $G_t$ as shown in Fig. 1 at 20 °C, pH 7.5. $K_{eq}^{-G}$ is defined as the ratio of [MII]/[MI], whereas $K_{eq}^{+G}$ is defined as the ratio of ([MII]+[MII-$G_t$])/[MI].

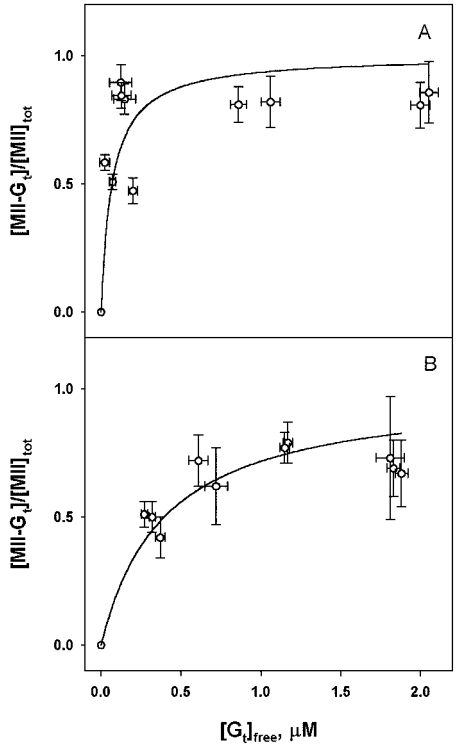


FIG. 3. **Lipid dependence of MII-$G_t$ binding.** The smooth lines are best fits of Equation 2 to the data. *A* and *B*, 18:0,22:6PC (*A*) and 18:0,18:1PC (*B*) with 30 mol% cholesterol at 20 °C, pH 7.5.

the MII peaks in both bilayer systems (Fig. 1, *A* and *B*, *filled circles*). This is the result of MII-$G_t$ complex formation and the fact that formation of this complex does not alter the spectral properties of MII.

The spectral contribution of the bands with absorption peaks centered at 480 nm and 385 nm in Fig. 1 (*A* and *B*) were deconvolved into contributions as a result of MI and MII in the absence of $G_t$ and MI and (MII + MII-$G_t$) in the presence of $G_t$, as shown by *dashed* and *solid curves*, respectively. It is clear that the amount of MII or (MII + MII-$G_t$) formed was greater in 18:0,22:6PC relative to 18:0,18:1PC with 30 mol% cholesterol, demonstrating the role of lipid composition in modulating the formation of MII and MII-$G_t$. The calculated values of $K_{eq}^{-G}$ and $K_{eq}^{+G}$ in 18:0,22:6PC (Fig. 1*A*) were 1.01 ± 0.02 and 2.22 ± 0.14, respectively, whereas $K_{eq}^{-G}$and $K_{eq}^{+G}$ in 18:0,18:1PC with 30 mol% cholesterol (Fig. 1*B*) were 0.19 ± 0.04 and 0.35 ± 0.04, respectively.

Both $K_{eq}^{-G}$ and $K_{eq}^{+G}$ varied by more than a factor of 5 over the range of bilayer compositions examined in this study, as shown in Fig. 2. In the absence of $G_t$, $K_{eq}^{-G}$ followed the order of di22:6PC > 18:0,22:6PC > 18:0,22:6PC + 30 mol% cholesterol ≈ 18:0,18:1PC > 18:0,18:1PC + 30 mol% cholesterol. This is consistent with previous findings (25–29) that showed that the reduced acyl chain unsaturation and the presence of cholesterol reduce the equilibrium concentration of MII. The presence of $G_t$ increased the apparent amount of MII formed in all samples, as indicated by the values of $K_{eq}^{+G}$. This results from the formation of the MII-$G_t$ complex. The trend for $K_{eq}^{+G}$ with bilayer composition followed that of $K_{eq}^{-G}$.

Values of $[G_t]_{free}$, [MII-$G_t$], and [MII] were calculated from $K_{eq}^{-G}$ and $K_{eq}^{+G}$ according to Equations 3–5. A series of measurements made with increasing ratios of $G_t$ to MII was used to produce the binding profiles of MII to $G_t$. Example plots of $[MII\text{-}G_t]/[MII]_{total}$ *versus* $[G_t]_{free}$ in two lipid compositions are shown in Fig. 3. Increased concentrations of $G_t$ resulted in an increase amount of MII-$G_t$ complex formation. However, the slopes in the binding plots were rather different, reflecting dissimilar binding constants in the two lipid bilayers. Analysis of the data according to Equation 2 gave $K_a$ of $1.5 \times 10^7$ $M^{-1}$ for 18:0,22:6PC vesicles and $K_a$ of $2.5 \times 10^6$ $M^{-1}$ for 18:0,18:1PC vesicles containing 30 mol% cholesterol.

Both acyl chain unsaturation and cholesterol content modulated the binding of MII to $G_t$ as shown in Fig. 4. Two key observations may be drawn from the values of $K_a$. 1) The increase in acyl chain unsaturation going from 18:0,18:1PC to 18:0,22:6PC resulted in a 3-fold enhancement in $K_a$, whereas further increase in unsaturation going to di22:6PC resulted in a slight reduction in $K_a$ relative to 18:0,22:6PC. 2) Cholesterol reduced $K_a$ in both monounsaturated 18:0,18:1PC and highly unsaturated 18:0,22:6PC. The $K_a$ values in 18:0,18:1PC + 30 mol% cholesterol and 18:0,22:6PC + 30 mol% cholesterol are $2.5 \times 10^6$ $M^{-1}$ and $4.4 \times 10^6$ $M^{-1}$, respectively, showing a somewhat smaller effect in the polyunsaturated bilayer.

## DISCUSSION

Previous studies have demonstrated that the formation of the active conformation of the G protein-coupled receptor rhodopsin, MII, is dependent on the membrane lipid composition (23;25–29), consistent with the present results regarding the lipid dependence of $K_{eq}^{-G}$. A primary finding of this study is that MII-$G_t$ complex formation, the initial amplification step in the visual cascade, is also modulated by the phospholipid acyl chain and cholesterol composition of the membrane. Increased acyl chain unsaturation and decreased level of cholesterol resulted in a higher affinity of MII to $G_t$. One characteristic of the native disc membrane is that ~50% of the total acyl chains are made of 22:6*n*-3, which is similar to that in 18:0,22:6PC. The reported $K_a$ in native disc is on the order of $10^7$ $M^{-1}$ (30, 31), whereas $K_a$ in 18:0,22:6PC reconstituted vesicles is $1.5 \times 10^7$ $M^{-1}$. The agreement between these values, despite the differences in phospholipid headgroup composition, indicates the important role of 22:6*n*-3 in modulating the coupling of rhodopsin to $G_t$.

Increased phospholipid acyl chain unsaturation was shown to increase the formation of MII (27, 29), whereas increased

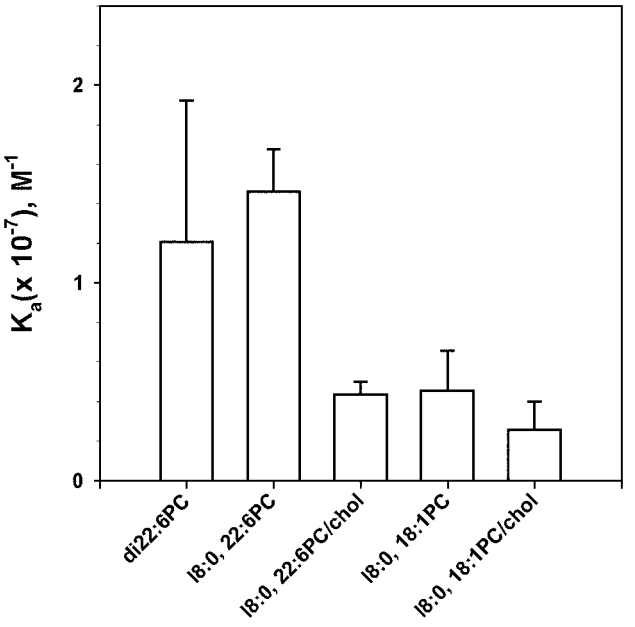


FIG. 4. **Effect of lipid composition on $K_a$ of MII-$G_t$.** The values are derived from data similar to that shown in Fig. 3 at 20 °C, pH 7.5.

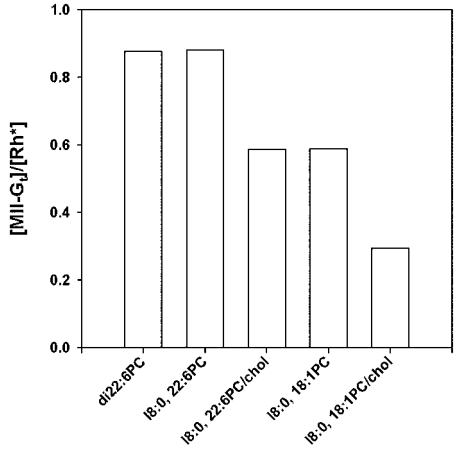


FIG. 5. **Calculated yield of MII-$G_t$ formed relative to the number of rhodopsin molecules that absorbed a photon at physiological light levels.** [MII-$G_t$]/[Rh*] was calculated according to Equation 6 using experimentally determined values of $K_{eq}^{-G}$ and $K_a$. The concentrations of rhodopsin and $G_t$ were set at 10 and 1 $\mu$M, respectively. The physiological bleach level for rhodopsin was assumed to be 1 of 100,000.

cholesterol concentration decreases MII (28). These findings have been linked to the specific packing properties of polyunsaturated acyl chains and the effect of cholesterol on these packing properties (29). Current evidence indicates that MII-$G_t$ interactions involve the three hydrophilic loops on the cytoplasmic surface of rhodopsin with regions in the carboxyl-terminal region of $G_t$, placing the interaction surfaces external to the bilayer. The dependence of the extent of MII-$G_t$ complex formation on the phospholipid acyl chain composition demonstrates that membrane lipid composition can not only play a role in modulating the level of MII formation, but it has a marked effect on the coupling of an integral membrane protein receptor to a peripherally bound G protein. Hence, the acyl chain packing in the hydrophobic region of the bilayer can affect interactions thought to occur primarily in the hydrophilic region of integral and peripheral membrane proteins.

Our results demonstrate that acyl chain composition and cholesterol content modulate the coupling step of $G_t$ to MII. To understand how lipid composition may modulate MII-$G_t$ interactions, it is necessary to consider the molecular events associated with MII-$G_t$ binding. The formation of the MII-$G_t$ complex involves a diffusional search of MII and $G_t$ for each other on the membrane surface and subsequent productive collisions leading to binding. Varying phospholipid acyl chain composition and cholesterol content can alter membrane properties in a number of ways. 1) Acyl chain packing properties can affect the rotation and diffusion of rhodopsin in the membrane. 2) The lateral diffusion and association of $G_t$ on the membrane can be changed. $G_t$ is associated with the membrane through an isoprenoid linkage. Acyl chain packing may affect the orientation of $G_t$ in the bilayer making MII-$G_t$ collisions less productive in terms of complex formation. 3) Increased acyl chain saturation inhibits the formation of MII because the outward movement of helices during MII formation may be hindered in a more rigid lipid environment resulting in reduced MII-$G_t$ complex formation. In addition, the sensitivity to acyl chain and cholesterol content may indicate a greater role of protein-protein interactions within the hydrophobic portion of the membrane than were considered previously. In a separate study, the effect of lipid composition on the kinetics of MII and MII-$G_t$ formation was studied using flash photolysis (32). We found that the kinetics of MII formation, which is a unimolecular reaction, exhibited relatively mild dependence on bilayer composition, whereas the kinetics of MII-$G_t$ formation was greatly diminished by the presence of cholesterol and more saturated lipids. These findings support the role of lipid composition in modulating the diffusional coupling of MII to $G_t$ on membrane surface.

Visual signaling is initiated from rhodopsin and propagated along the visual cascade through a series of coupled steps. In this study we have demonstrated that the initial steps, which are rhodopsin activation and MII-$G_t$ coupling, are modulated by lipid composition and cholesterol. The net effect of bilayer composition on visual transduction can be evaluated in terms of the yield of MII-$G_t$ complex formation per bleached rhodopsin, [MII-$G_t$]/[Rh*]. The following equation was used for such calculation.

$$\frac{[\mathrm{MII}-G_t]}{[\mathrm{Rh}^*]} = \frac{m - \sqrt{m^2 - 4\cdot K_a^2\cdot \mathrm{Rh}^*\cdot[G_t]}}{2\cdot K_a\cdot[\mathrm{Rh}^*]}, \qquad \text{(Eq. 6)}$$

where $[G_t]$ is the total concentration of $G_t$, and

$$m = (1 + 1/K_{eq}^{-G}) + K_a\cdot[G_t] + [\mathrm{Rh}^*]\cdot K_a. \qquad \text{(Eq. 7)}$$

Equation 6 is derived from the following equations.

$$K_{eq}^{-G} = [\mathrm{MII}]/[\mathrm{MI}] \qquad \text{(Eq. 8)}$$

$$K_a = [\text{MII-G}_t]/([\mathrm{MII}]\cdot([G_t] - [\text{MII-G}_t])) \qquad \text{(Eq. 9)}$$

$$[\mathrm{Rh}^*] = [\mathrm{MI}] + [\mathrm{MII}] + [\text{MII-Gt}] \qquad \text{(Eq. 10)}$$

Under physiological conditions, the ratio of rhodopsin to $G_t$ is ~10 to 1 in ROS membranes and in the range of 1 of 100,000 rhodopsins absorbs a photon, giving rise to a visual response. The effect of bilayer composition on [MII-$G_t$]/[Rh*] is clearly demonstrated in Fig. 5. Although ~90% of bleached rhodopsin formed complex with $G_t$ in 18:0,22:6PC and di22:6PC vesicles, only 60% of such complex is formed in 18:0,18:1PC vesicles. The presence of 30 mol% cholesterol in 18:0,22:6PC and 18:0,18:1PC resulted in ~60 and 30% complex formation, respectively. It was recently reported that ~10% of rhodopsin in the ROS disc membrane is contained in a detergent-resistant membrane fraction or lipid raft (33). If this raftlike phase exists under physiological conditions, and like other lipid rafts, it is rich in cholesterol and saturated acyl chains, the present results sug-

gest that MII-$G_t$ binding strength and kinetics would be reduced for this population of rhodopsin. In addition to phosphatidylcholine, the native disc membrane also contains ~10% phosphatidylserine (PS) and ~42% phosphatidylethanolamine (PE) (1). PS will add a negative surface charge to the membrane, whereas PE will contribute an increased level of acyl chain packing order because of its higher melting point relative to PC. Our current data would suggest that the presence of PE would be somewhat inhibitory relative to MII-$G_t$ complex formation. The effect of PS is yet to be determined.

A model, relating the biochemical events in the visual transduction pathway with the neural response, as measured by the electroretinograms, was recently published (34). In this model, the response at any time after a light stimulus is directly proportional to the concentration of activated rhodopsin molecules, *i.e.* [MII]. Here, we have determined that, at very low light levels, the fraction of MII-$G_t$ complex to bleached rhodopsin, [MII-$G_t$/Rh*] depends on the lipid composition of the membrane, Fig. 5. If [MII-$G_t$/Rh*] is a measure of the fraction of bleached rhodopsin that can participate in activating $G_t$, then the factor in the equation for the response time at physiological light exposures needs to be corrected for variation in membrane lipid composition. Both the 22:6*n*-3-containing PCs examined in this study support nearly full participation of the bleached rhodopsin in $G_t$ activation, Fig. 5. In contrast, the 18:1*n*-9-containing PC supports only 60% participation of the bleached rhodopsin in $G_t$ activation, whereas the addition of 30 mol% of cholesterol reduces this to about 30%. Thus, the response time in the 22:6*n*-3-containing PC's would be expected to be faster relative to that observed in the 18:1*n*-9-containing PC by a factor of 1.67. In the case of *n*-3 deficiency, 22:6*n*-3 is replaced by a lower level polyunsaturated, 22:5*n*-6, and a lag time is observed in the leading edge of the a-wave in the electroretinograms (35). Decreased MII participation in MII-$G_t$ complex formation would also contribute to lower signal amplitude, because fewer $G_t$ proteins would be activated. Although, it is not anticipated that the difference between 22:6*n*-3 and 22:5*n*-6 will produce as great a lag time as is indicated for 18:1*n*-9, the observed lag time and reduced signal amplitude in *n*-3 deficiency relative to *n*-3-sufficient subjects is consistent with the dependence of the level of MII-$G_t$ complex formation on the membrane lipid composition.

The visual cascade, initiated by the light activation of rhodopsin, involves a series of protein-coupled reactions resulting in an amplified response. The first step in signal amplification in the visual pathway is the formation of the MII-$G_t$ complex. The modulatory effect of bilayer acyl chain composition and cholesterol content on both the kinetics and extent of formation of the MII-$G_t$ complex observed in this and the previous (32) study will have direct impact on the downstream steps of the visual cascade. Weakened MII-$G_t$ interactions will results in reduced amplification and slower kinetics at the $G_t$ activation step, which will propagate down the pathway to produce reduced activity of the effector protein, cGMP phosphodiesterase. These effects may well provide the molecular basis for the diminished amplitude and sensitivity (36, 37) and lag time in the electroretinogram a-wave (35) and the reduced visual acuity (38) associated with 22:6*n*-3 deficiency. Because of the similar signaling motif in other G protein-coupled signaling systems, the findings in this study should be generally applicable to other members in the G protein-coupled family, providing a molecular mechanism for the observed loss in cognitive skills (2), odor (4), and spatial discrimination (5) observed in *n*-3 fatty acid deficiency.

REFERENCES


1. Stinson, A. M., Wiegand, R. D., and Anderson, R. E. (1991) *Exp. Eye Res.* **52,** 213–218
2. Salem, N. (1989) in *New Protective Roles for Selected Nutrients* (Spiller, G. A., and Scala, J., eds) pp. 109–228, Alan R. Liss Inc., New York
3. Birch, E. E., Birch, D. G., Hoffman, D. R., and Uauy, R. (1992) *Invest. Ophthalmol. Vis. Sci.* **33,** 3242–3253
4. Greiner, R. S., Moriguchi, T., Hutton, A., Slotnick, B. M., and Salem, N. (1999) *Lipids* **34,** (suppl.) S239–S243
5. Moriguchi, T., Greiner, R. S., and Salem, N. (2000) *J. Neurochem.* **75,** 2563–2573
6. Helmreich, E. J., and Hofmann, K. P. (1996) *Biochim. Biophys. Acta* **1286,** 285–322
7. Matsuda, T., Takao, T., Shimonishi, Y., Murata, M., Asano, T., Yoshizawa, T., and Fukada, Y. (1994) *J. Biol. Chem.* **269,** 30358–30363
8. Kisselev, O. G., Ermolaeva, M. V., and Gautam, N. (1994) *J. Biol. Chem.* **269,** 21399–21402
9. Seitz, H. R., Heck, M., Hofmann, K. P., Alt, T., Pellaud, J., and Seelig, A. (1999) *Biochemistry* **38,** 7950–7960
10. Ernst, O. P., Meyer, C. K., Marin, E. P., Henklein, P., Fu, W. Y., Sakmar, T. P., and Hofmann, K. P. (2000) *J. Biol. Chem.* **275,** 1937–1943
11. Farahbakhsh, Z. T., Ridge, K. D., Khorana, H. G., and Hubbell, W. L. (1995) *Biochemistry* **34,** 8812–8819
12. Litman, B. J., and Mitchell, D. C. (1996) in *Biomembranes* (Lee, A., ed) pp. 1–32, JAI Press, Greenwich, CT
13. Hargrave, P. A., and McDowell, J. H. (1992) *FASEB J.* **6,** 2323–2331
14. Sakmar, T. P. (1998) *Prog. Nucleic Acid Res. Mol. Biol.* **59,** 1–34
15. Mathews, R., Hubbard, R., Brown, P., and Wald, G. (1963) *J. Gen. Physiol.* **47,** 215–222
16. Hofmann, K. P. (1985) *Biochim. Biophys. Acta* **810,** 278–281
17. Hamm, H. E. (1998) *J. Biol. Chem.* **273,** 669–672
18. Konig, B., Arendt, A., McDowell, J. H., Kahlert, M., Hargrave, P. A., and Hofmann, K. P. (1989) *Proc. Natl. Acad. Sci. U. S. A.* **86,** 6878–6882
19. Franke, R. R., Konig, B., Sakmar, T. P., Khorana, H. G., and Hofmann, K. P. (1990) *Science* **250,** 123–125
20. Palczewski, K., Kumasaka, T., Hori, T., Behnke, C. A., Motoshima, H., Fox, B. A., Le, T., I, Teller, D. C., Okada, T., Stenkamp, R. E., Yamamoto, M., and Miyano, M. (2000) *Science* **289,** 739–745
21. Franke, R. R., Sakmar, T. P., Graham, R. M., and Khorana, H. G. (1992) *J. Biol. Chem.* **267,** 14767–14774
22. Emeis, D., Kuhn, H., Reichert, J., and Hofmann, K. P. (1982) *FEBS Lett.* **143,** 29–34
23. Straume, M., Mitchell, D. C., Miller, J. L., and Litman, B. J. (1990) *Biochemistry* **29,** 9135–9142
24. Boesze-Battaglia, K., and Albert, A. D. (1990) *J. Biol. Chem.* **265,** 20727–20730
25. Litman, B. J., and Mitchell, D. C. (1996) *Lipids* **31,** (suppl.) S193–S197
26. Brown, M. F. (1994) *Chem. Phys. Lipids* **73,** 159–180
27. O'Brien, D. F., Costa, L. F., and Ott, R. A. (1977) *Biochemistry* **16,** 1295–1303
28. Mitchell, D. C., Straume, M., Miller, J. L., and Litman, B. J. (1990) *Biochemistry* **29,** 9143–9149
29. Mitchell, D. C., Straume, M., and Litman, B. J. (1992) *Biochemistry* **31,** 662–670
30. Kuhn, H., Bennett, N., Michel-Villaz, M., and Chabre, M. (1981) *Proc. Natl. Acad. Sci. U. S. A.* **78,** 6873–6877
31. Parkes, J. H., Gibson, S. K., and Liebman, P. A. (1999) *Biochemistry* **38,** 6862–6878
32. Mitchell, D. C., Niu, S., and Litman, B. J. (2001) *J. Biol. Chem.* **276,** 42801–42806
33. Seno, K., Kishimoto, M., Abe, M., Higuchi, Y., Mieda, M., Owada, Y., Yoshiyama, W., Liu, H., and Hayashi, F. (2001) *J. Biol. Chem.* **276,** 20813–20816
34. Leskov, I. B., Klenchin, V. A., Handy, J. W., Whitlock, G. G., Govardovskii, V. I., Bownds, M. D., Lamb, T. D., Pugh, E. N., and Arshavsky, V. Y. (2000) *Neuron* **27,** 525–537
35. Neuringer, M., Connor, W. E., Van Petten, C., and Barstad, L. (1984) *J. Clin. Invest.* **73,** 272–276
36. Weisinger, H. S., Vingrys, A. J., and Sinclair, A. J. (1996) *Lipids* **31,** 65–70
37. Weisinger, H. S., Vingrys, A. J., Bui, B. V., and Sinclair, A. J. (1999) *Invest. Ophthalmol. Vis. Sci.* **40,** 327–338
38. SanGiovanni, J. P., Parra-Cabrera, S., Colditz, G. A., Berkey, C. S., and Dwyer, J. T. (2000) *Pediatrics* **105,** 1292–1298